

# Stacked Wolfcamp Laterals



# Improve Pad Drilling And Completion Economics

By Michael Shoemaker,

Nancy Zakhour and Joshua Peacock

HOUSTON—The thickness of the Wolfcamp Shale is unique among North American tight oil formations. Exceeding 2,500 feet in places, the Wolfcamp's thickness allows for multiple zones of stacked low-permeable pays, translating into millions of additional acres of potential horizontal development when defined in 3-D space.

As part of its ongoing effort to optimize completion methods, develop future "stacked lateral" field development strategies, and high-grade exploratory Wolfcamp landing zones from 3-D seismic data, Callon Petroleum Company integrated numerous multidisciplinary measurements on three horizontal laterals in the Southern Midland Basin in West Texas. Drilled in a chevron pattern with stacked laterals vertically spaced at minimal distances, two of the horizontals targeted the deeper Wolfcamp B formation and the other targeted the Wolfcamp A.

This empirical approach demonstrates the integration of multidisciplinary measurements to optimize completion parameters with lower costs using stage-by-stage analysis, and to improve fracture modeling workflows for a more complete and accurate solution for optimizing production rates.



The three laterals were stimulated in a simultaneous zipper frac sequence with geometric stage placement. Real-time microseismic monitoring was used to observe the treatments and the resulting heights and lateral extent of the hydraulic fractures. Although identical pumping schedules were intended initially for all three laterals, it became apparent during the treatments that microseismic height growth varied significantly across the laterals within individual stages.

Linear regression analyses showed strong correlations between seismic P-wave impedance versus microseismic data and fracture pressure responses, shale mineralogy compositions, and geomechanical properties calculated from core-supported petrophysical data. Mineralogical and geomechanical shale properties were measured directly from 3-D surface seismic data lengthwise along lateral trajectories at individual frac stages.

The results indicate that microseismic fracture height variability in the three wells was influenced most by changes in shale stratigraphy and mineralogy composition, without a definitive relationship with treatment injection rates. Optimal fracture heights were observed in landing areas with significant volumes of calcite (Vcal), characteristic of high Young's modulus and closure stress (variables estimated from 3-D seismic).

For validation, the production histories of the three laterals and numerous other wells in the field confirm a strong correlation between inverted seismic P-wave impedance and initial 120-day cumulative oil in landing zones with high Vcal (brittleness) and correspondingly low clay.

### Wolfcamp Geology

Callon Petroleum is focused on onshore unconventional oil and natural gas reserves, with its asset base concentrated in the Midland Basin. Its operations are focused on horizontal drilling in several prospective intervals, including multiple levels of the Wolfcamp and Spraberry formations. The company operates two horizontal drilling rigs focused on five prospective development zones.

Wolfcamp laterals are typically 5,000-10,000 feet long. The lower costs associated with drilling stacked horizontals in a chevron pattern from pads (Figure 1) improves economics, while simultaneously completing multiple wells in a zipper sequence increases stimulation efficiency and achieves higher initial production rates. Obviously, increased production is particularly critical during periods of low crude oil prices.

The Wolfcamp formation has four independent landing zones in the Upton County, Tx., area of the Southern Midland Basin: the A, B, C and D (or Cline). Each

zone is well within the oil window, and contains varying volumes of mineral compositions, including quartz, limestone, clay and kerogen. In this three-well project, microseismic data were acquired for the Wolfcamp A and B zones only.

The Wolfcamp B generally has relatively higher initial production rates and greater estimated ultimate recoveries than the other zones, given its ideal mineralogy for enhanced brittleness and greater oil saturations. The Wolfcamp A typically contains massive carbonate detrital deposits toward its base that can act as fracture barriers. The C and D zones are deeper in the section and have higher fracture gradients. They are increasingly influenced by deeper-seated structures that potentially can induce geosteering challenges.

For all four zones, mineralogy compositions define the mechanical layers that are most prone to fracturing, which is a function of changes in lateral and vertical depositional (mineralogical) facies. Wolfcamp mineralogy varies considerably across the Midland Basin, as demonstrated by petrophysical logs acquired in vertical wellbores.

Geologically, Wolfcamp rocks in the central and southern parts of the basin are characteristic of kerogen-rich dark shales and interbedded detrital carbonates, muds, sands and silts that were deposited predominantly by debris/gravity flows and turbidity currents downslope from the Central Basin Platform (CBP), likely in a proximal basin plain environment. Shelf-ward toward the CBP, carbonate deposition increases to a point where large detached blocks of dolostone are common proximal to the platform margin.

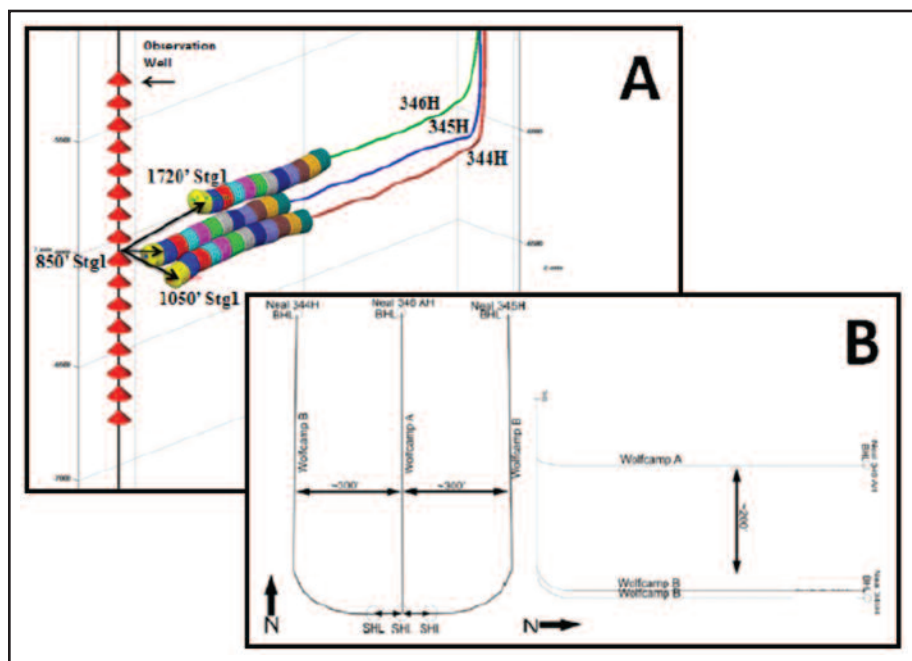
Consequently, the abundance and distribution of carbonate-rich detrital flows can be used as a proxy in determining relative distance from the CBP margin, which in turn, defines carbonate fairways prone to fracture stimulation for increased production when high grading acreage for development.

### Two Distinct Units

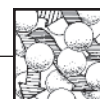
Each Wolfcamp zone can be subdivided into two units: a high clay volume (Vclay) ductile "flooding surface" interval, which saw minimal carbonate shedding, and a more brittle calcite-rich carbonate "bench" interval. Operators typically land laterals below the flooding surface and within the more brittle carbonate bench to optimally initiate wide hydraulic fracture networks near the wellbore. This allows for

FIGURE 1

Stacked Laterals in Chevron Pattern (A) And Wolfcamp A and B Well Spacing (B)







fracture propagation and proppant embedment into the relatively ductile flooding surface above, which typically has more oil saturation and kerogen content.

Unlike the relatively ductile flooding surface, the carbonate bench is more fracture-prone with higher Vcal, which correlates strongly to a dynamic Young's modulus (the rock's ability to maintain a fracture). Poisson's ratio also is a key mechanical property that quantifies the rock's ability to fail under stress. When combined, these variables define the rock's "fracability," in this case, expressed as a brittleness index calculated using the p-sonic and dipole logs from the Neal 307 offset pilot hole.

Clay volume is crucial in brittleness index correlations. Brittleness decreases as calcite is subtracted and replaced by Vclay, increasing ductility. A general rule of thumb in shale plays is that the lower the Poisson's ratio and the higher the Young's modulus, the more brittle and fracture competent the rock becomes. Poisson's ratio and quartz (which is brittle and prone to fracturing) both show minimal variability throughout the Midland Basin, making them poor proxies for characterizing Wolfcamp brittleness.

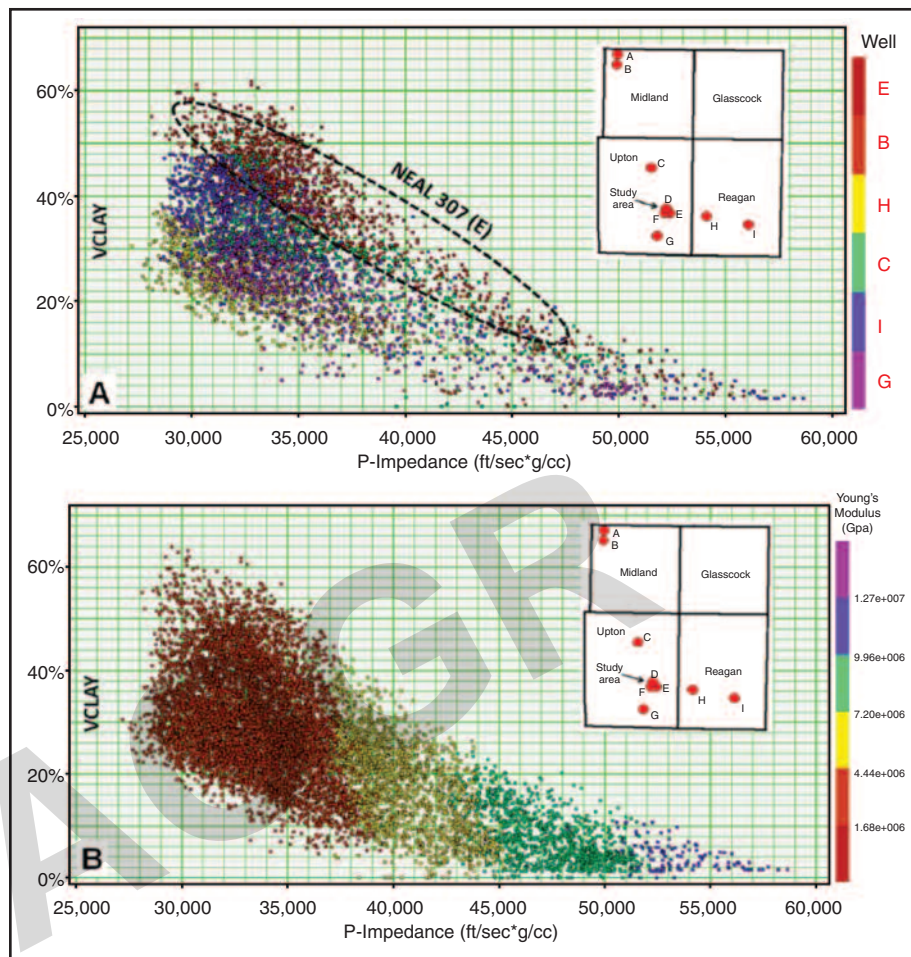
As shown in the cross plots in Figure 2, however, strong correlations do exist basinwide between Vclay and Young's modulus, in addition to acoustic p-impedance. Specifically, as Vclay decreases and is replaced by Vcal, Young's modulus increases linearly with increasing values of p-impedance rock property measurements estimated directly from inverted 3-D surface seismic.

The analysis shows a good correlation between initial 120-day cumulative production from adjacent laterals in the field and average p-impedance extrapolated lengthwise along each of the well trajectories. Higher producing wells correlate to higher magnitudes of p-impedance, where Vcal is interpreted to exist to create higher brittleness values and more efficient fracture stimulation.

Better producing wells are located in the extreme northwest quadrant of the field (Figure 3), where a carbonate-rich (detrital) lobe has been confirmed by petrophysical logs in vertical wellbores.

Consequently, a high degree of vertical and lateral heterogeneity exists within the Wolfcamp that is geology-driven and associated with the irregular stacking of discrete depositional carbonate units. The result is varying mineralogy compositions

**FIGURE 2**  
Regional Well Cross-Plots of P-Impedance and B Bench Vclay (A) And Young's Modulus for Wolfcamp A and B (B)



that ultimately define and correlate with geomechanical properties characterized by relative fracability and brittleness. These mechanical properties ultimately influence fracture stimulation geometries, including hydraulic fracture height and half-length, which require calibration to microseismic and completion data.

### Inverted Seismic Impedance

The normal-incidence, post-stack 3-D surface seismic data were acquired with 82.5-foot bin spacing, and were processed for zero phase to preserve relative amplitude. The 3-D data were inverted to p-impedance, resulting in seismic-derived rock property units that could be integrated and correlated with petrophysical and geomechanical dipole logs as well as microseismic data.

The seismic inversion process included deterministic wavelet estimation to ensure zero-phase data for peak-energy seismic response at acoustic interfaces to ex-

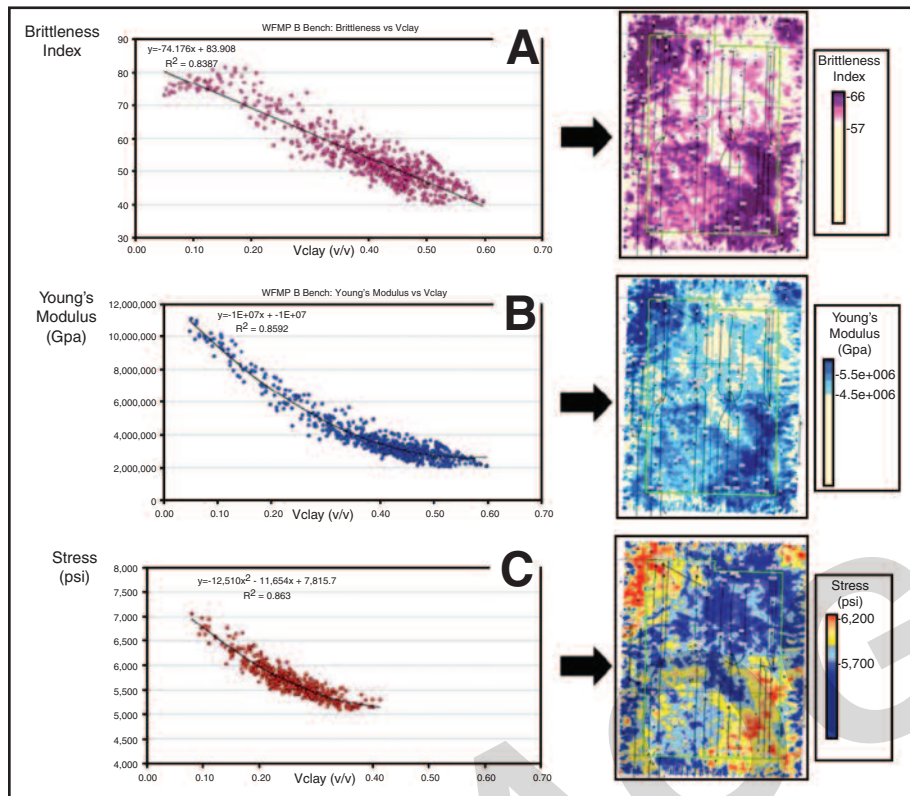
trapolate accurate p-impedance maps. Mixed- or rotated-phase data would have resulted in varying energy distributions across amplitude events, leading to inaccurate results not characteristic of true stratigraphic and mineralogical variabilities.

Because of the high volume of calcite, the seismic response to bench horizons is represented by a p-impedance amplitude peak converse to clay-rich flooding surfaces (low impedance amplitude troughs). The relative thickness of the Wolfcamp A and B bench and flooding surface are well within the resolvable limits of the seismic data, as is lateral resolution (Fresnel-zone), which was essential when extrapolating pseudo-lateral logs from the seismic.

To capture local lateral variability in rock properties, zone-wise cross plots of p-impedance versus Vclay, Vcal, Young's modulus and closure stress were created for the Wolfcamp A and B from dipole and p-sonic logs from the Neal 307 offset vertical well. The cross plots showed strong



**FIGURE 3**  
**Zone-Wise Correlations Between Vclay and Brittleness Index (A),**  
**Young's Modulus (B) and Closure Stress (C)**



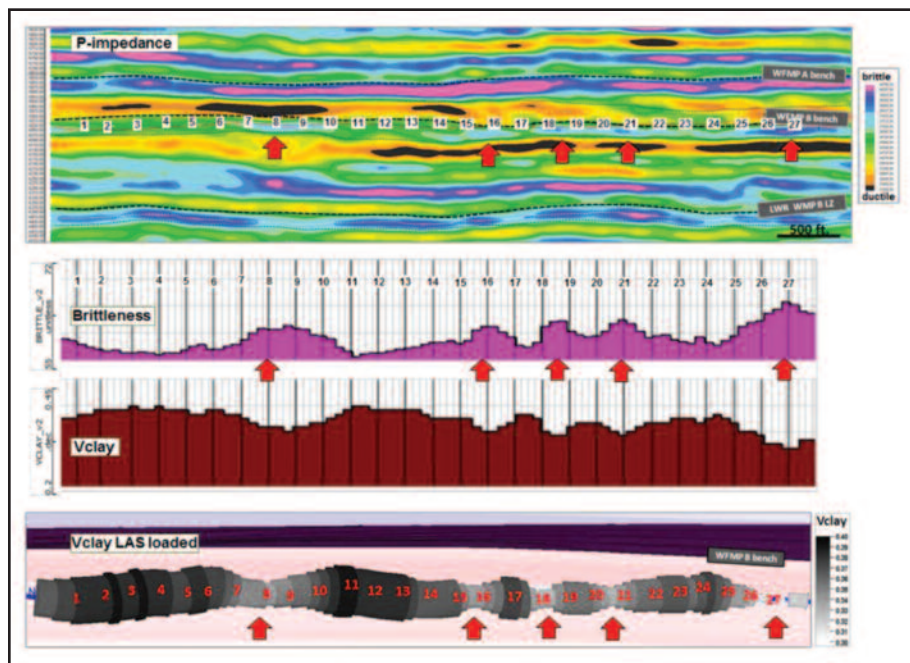
correlations, resulting in linear transform functions that were used to create the mineralogical and geomechanical seismic volumes of each property.

Zone-wise attribute maps of the correlations were generated to enable the direct extrapolation of properties lengthwise along the wellbores in creating seismic pseudo-lateral logs. Figure 3 shows strong correlations among Vclay and brittleness index, Young's modulus, and closure stress. The linearity of the geomechanical properties confirms that replacing Vclay with Vcal results in greater fracability.

The extrapolated pseudo-Vclay log created from the workflow (Figure 4, with the arrows indicating minimal Vclay for optimal fracture stimulation) was followed by reformatting a full suite of logs to a log ASCII standard file for inputting into fracture modeling software. This enabled surface seismic rock properties nearest the lateral (where microseismic and completion data were acquired) to be modeled versus data interpolated significant distances from the study area.

A more detailed and unique stage-by-stage analysis using the surface seismic impedance could be integrated now with completion data, microseismic data, and fracture models for "smart" frac analysis to determine optimal stimulation and completion parameters on future wells.

**FIGURE 4**  
**Vclay Pseudo Lateral Log Extrapolated**  
**From 3-D Seismic Lengthwise along the Neal 345H**



**Microseismic Interpretation**

The Neal 346AH was landed in the Wolfcamp A bench and treated first, followed by the 345H and 344H wells in the Wolfcamp B. As part of the simultaneous zipper fracturing process, an identical hydraulic fracturing treatment pump schedule was designed for all three laterals, using geometrical completion spacing. The pump schedule consisted of slickwater with 100-mesh sand and 40/70-mesh white sand.

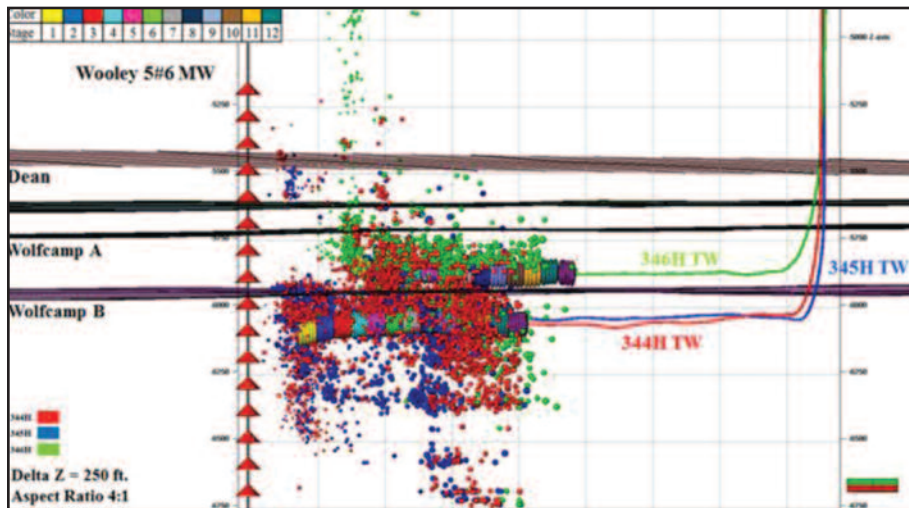
Treatment parameters were adjusted using real-time microseismic to control excessive height growth. The main concern was completing stages 4 and onward toward the heel of the wells—particularly the deeper Wolfcamp B wells—since they were aligned with the shallower Wolfcamp A stages and potentially could lead to interference issues between developed fractures.

The first 12 toe-ward stages of each of the laterals were monitored using a 16-receiver downhole array deployed in the vertical section of the Woolley 5 No. 6 monitor well. The rest of the stages were not monitored, given the increasing distance





**FIGURE 5**  
**Depth View of Microseismic Events Colored by Well**  
**And Sized by Magnitude (All Three Laterals)**



and longer offsets from the receiver array.

With identical stimulation designs, microseismic distribution with the hydraulic fracture geometry was expected to be relatively consistent from one stage to the other in each lateral. However, the microseismic data showed the stages treating very differently. Figure 5 presents a depth view of microseismic activity, with events colored by well.

Treatment slurry rates were adjusted throughout the real-time fracturing operations to limit upward microseismic height growth observed on some of the stages. The observed microseismic event depths indicate that despite real-time variations in stimulation treatment rates to control microseismic height development, the microseismic distribution did not display consistent behavior with the changes implemented. There were clear variations in height growth in the first 12 stages of the Neal 345H.

To investigate microseismic variations in developed fracture geometry, geomechanical and petrophysical log measurements from the Neal 307 offset (located less than a half mile away) were compared with the microseismic distribution in stages 1-12 in the Neal 345H. The upper boundary that potentially limits upward fracture height growth and microseismic activity appeared variable from one segment of the lateral to the next. Downward growth showed more consistent change, with more stages completed and more microseismic downward growth for the stages toward the heel.

**Identifying Fracture Barriers**

Without a clear understanding of the lateral changes in rock properties at different depths, it becomes more challenging to determine variations in fracture treatment pressure responses, in addition to microseismic event distribution and source parameter. Potential fracture barriers were identified from Neal 307 vertical logs. The minimum in-situ stress was propagated across a 3-D geomechanical grid, taking into account the stratigraphic framework from 3-D seismic (Figure 6).

Since numerous fracture barriers could be identified by examining the contrast from low- to high-stress regions, the mi-

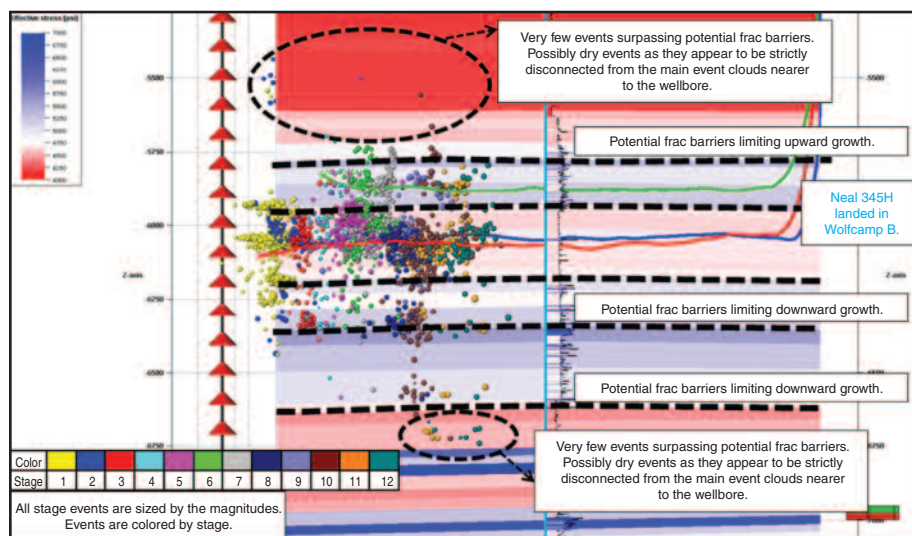
croseismic height growth distribution remained inconclusive. The zone-wise consistent, laterally interpolated stress profile appeared to match microseismic height only on a few stages, and failed to capture the lateral facies variability influencing microseismic fracture response.

Figure 7A shows treatment results from the fifth stage of the Neal 345H. The image at top left shows microseismic events in map view colored by time and sized by magnitudes. Microseismic events in depth view against a zoned stress profile are shown at top right. The bottom graph shows the treatment plot with surface pressure (red), treatment slurry rate (blue), proppant concentration (green), microseismic event rate (bars), microseismic event count (purple), and microseismic cumulative moment (black curve).

The data indicate the majority of microseismic activity in stage 5 developed with upward height growth, where most of the event density was located within the lower-stress zones of the Wolfcamp B (above the wellbore). A few events propagated shallower into the Wolfcamp A, where the 346H lateral is located, and more dispersed events were scattered within deeper portions of the Wolfcamp B in both lower- and higher-stress zones. It is clear that this stage had relatively decent height confinement compared with the microseismic distribution on the other stages of the 345H lateral.

On the other hand, the stage 10 stimulation saw the majority of microseismic height growth (Figure 7B) occur down-

**FIGURE 6**  
**Neal 345H Microseismic Events by Stage**  
**Displayed Against a Zoned Stress Profile**





**FIGURE 7A**

**345H Stage 5 Treatment**



**FIGURE 7B**

**345H Stage 10 Treatment**



ward into deeper portions of the formation. The bulk of the event density was clustered within the lower-stress zones of the Wolfcamp B that correspond to lower-stress zones located beneath the wellbore, as opposed to above the wellbore as in stage 5. The time-dependent difference in the propagation of the microseismic distribution potentially could indicate changes in formation properties that are essentially driving the distribution, and potentially, fracture growth.

**Integrating The Data**

In an attempt to understand fracture geometry and its characterization from microseismic activity and extracted dimen-

sions, a 3-D fracturing simulation workflow was performed. For consistency purposes, there were no step-rate tests prior to stimulation or post-frac production logs to help determine the number of clusters taking fluid. All clusters were, therefore, assumed to be active. The simulation used identical pumping schedules for all stages, since the actual executed pump schedule did not deviate significantly from the initial design.

Simulation frac heights were relatively consistent for the majority of the stages. They also appeared to be more confined than the microseismic results. Toe-ward stages 1, 2, 3 and possibly 4 (none of which were aligned with stages from the shallow-

er 346AH), tended to show greater similarities between simulated and microseismic heights. The Wolfcamp A lateral appeared to have impacted the upward height growth. However, that observation did not apply to all the stages aligned across the 346AH and 345H laterals.

Although there was no clear correlation between the simulated fracture and microseismic heights, fracture heights were smaller and more confined than microseismic growth. To better understand this variability in geometry and unlock the potential of integrated data analysis, 3-D surface seismic measurements were integrated with the microseismic results and geomechanical properties.

Figures 8 and 9 show microseismic data with arbitrary p-impedance seismic cross-sections lengthwise along the 345H well's lateral trajectory. When combining the formation properties obtained from the inverted p-impedance, delineating lateral changes along the wellbore at different depths is essential to correlating variations in microseismic response and subsequent changes in the developed hydraulic fracture geometry. The parameters extrapolated from seismic can be used on a stage-by-stage basis.

Twofold criteria can be used when interpreting mineralogical and geomechanical data from surface seismic integrated with observed fracture propagation behavior from microseismic events. Incidentally, this also could be used as a means to high grade acreage for development.

The first criterion is delineating an ideal mechanical bench for landing that has higher impedance, and is characteristic of a high calcite volume and high Young's modulus for enhanced brittleness. This would result in efficient hydraulic fracture initiation of wide fracture networks nearest the wellbore to allow pumping optimal slurry rates, and embedding proppant

**FIGURE 8**

**Well 345H Microseismic Data with P-Impedance Cross-Sections**

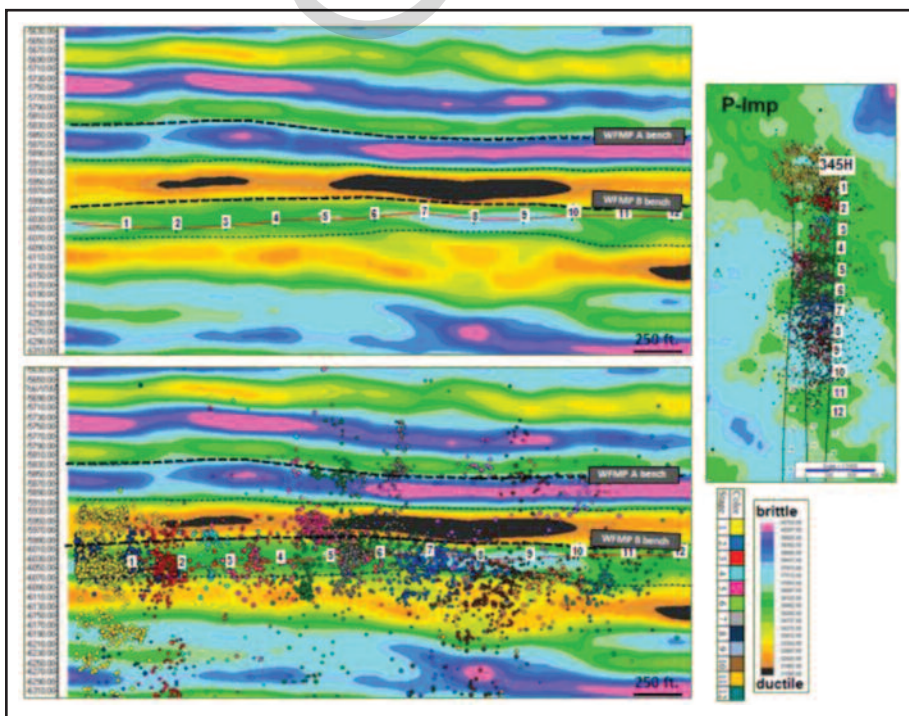
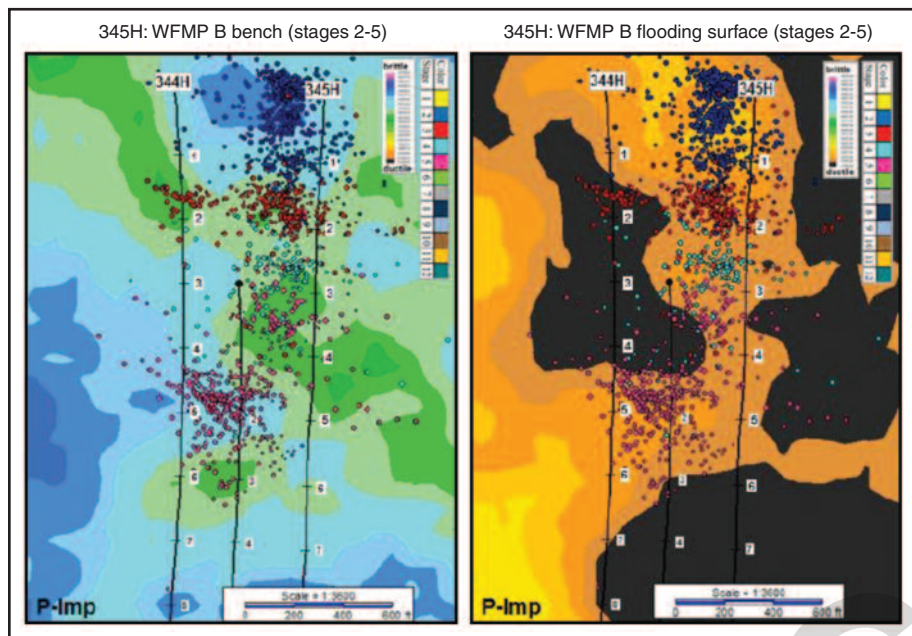






**FIGURE 9**  
**Stages 2-5 Microseismic Data with P-Impedance and Flooding Surface**



into the shallower flooding surface above.

The second criterion is for fracture containment in areas of greater ductility. This would include those areas that map flooding surfaces with significantly lower values of p-impedance for increased  $V_{clay}$  (and perhaps kerogen). Fracture containment becomes increasingly critical when implementing chevron-type patterns for stacked horizontal wells, and potentially could prevent the fracturing and “thieving” of oil production from adjacent pay zones.

### Well 345H Results

Investigating the first criterion shows a high density of microseismic events in stages 5 through 10, where the 345H was landed in an area of higher impedance (blue color in Figure 8). For the second criterion, the seismic event (flooding surface) above the landing bench is representative of particularly lower impedance from stages 5 through 10, and may act as a ductile barrier to contain fracture propagation within the zone.

Note that the microseismic heights at these stages are minimal and do not appear to extend into the Wolfcamp A zone above, from which the 346AH produces. The stage 5 microseismic events show greater heights, perhaps because of a less ductile overlying flooding surface at that location.

In addition, stage 5 microseismic events have an unusual geometry and subsequent fracture pattern. These events potentially demonstrate the propagating “front” of fractures aligning horizontally along the base of the flooding surface (and perhaps along natural fractures), and then propagating upward into the zone above as stress levels permit. The unique behavior of microseismic events in stage 5 also can be interpreted from the flooding surface map (the right panel in Figure 9). Stage 5 (pink) events appear to propagate away from lower impedance, or areas of higher ductility and less brittleness.

Stages 4-7 in the 344H Wolfcamp B lateral exhibited similar behavior, with microseismic events propagating away from areas of greater ductility until encountering higher brittleness. At that point, fracture heights appeared to increase significantly where a high number of microseismic events were recorded within the Wolfcamp A bench.

This study illustrates the high degree of geology-driven vertical and lateral heterogeneity that exists within the Wolfcamp formation. The irregular stacking of discrete depositional carbonate units results in varying mineralogy compositions that ultimately define and correlate with geo-mechanical properties characterized by relative fracability and brittleness. These mechanical properties ultimately influence

fracture stimulation geometries, including prop heights and half-lengths, which in turn, require calibration to microseismic and completions data.

The empirical approach Callon Petroleum Company deployed in the Midland Basin study demonstrates how multidisciplinary measurements can be integrated to successfully optimize completion parameters, improve fracture modeling workflows using seismic-derived rock properties, implement stage-by-stage smart frac analysis, and ultimately, improve production rates and development economics. □

**MICHAEL SHOEMAKER** is the chief geoscientist at Callon Petroleum and head of 3-D surface seismic operations, including data acquisition, processing, and geologic seismic interpretation for petrophysics/mineralogy, geomechanics and brittleness for optimal fracture stimulation of sweet spots. Before joining Callon Petroleum, Shoemaker was an exploration geophysicist at BP America, leading prospect generation in conventional onshore plays. Prior to that, he was an expatriate geophysicist working for various foreign companies located in the United Kingdom, United Arab Emirates and Malaysia, where he prospected for Petronas. Shoemaker holds a Ph.D. in geophysics from the University of Missouri-Rolla.

**NANCY ZAKHOUR** is a completion engineer at Callon Petroleum, focused on operational and technical completion optimization in the company’s Permian Basin assets. Prior to her current role, she worked at Schlumberger as a microseismic interpretation engineer and hydraulic fracturing engineer in North American unconventional shale plays. Zakhour holds a B.E. in electrical and computer engineering from the American University of Beirut.

**JOSHUA PEACOCK** is a geologist at Callon Petroleum, working in the company’s Permian Basin assets. He began his career at Energen Resources and has eight years of experience in the Permian Basin. Peacock holds a B.S.G. in geology from the University of Alabama.